Light Metals 2014
Edited by: John Grandfield
TMS (The Minerals, Metals & Materials Society), 2014

Properties of AlZn10Si8Mg Alloys for High Performances Application

Mario Rosso[1], Ildiko Peter[1], Christian Castella[1] Roberto Molina[2]

[1]Politecnico di Torino, Department of Applied Science and Technology, Institute of Science & Engineering of Materials for the Innovative technologies, ALTO – Metallurgy Group; ALessandria Campus & TOrino
Corso Duca degli Abruzzi, 24, 10129 Torino- Italy
[2]Teksid Aluminum Srl, Via Umberto II, 5, 10022 Carmagnola, Torino-Italy

Keywords: Al-based alloy, self-hardening, microstructure

Abstract

In this paper a self-hardening Al-based alloys (AlZn10Si8Mg) with potential application in automotive industry have been proposed.
Samples produced with different solidification rate have been considered. Mechanical strength, hardness evolution, morphological behaviour and corrosion resistance of the prepared samples with different content of Mg (in the range of 0.5÷3 wt%) have been investigated. Fracture surface analysis has been carried out to identify the presence of defects on the fractured surface and finally to correlate them to the mechanical performances.
As expected, higher solidification rate favours the development of the finest microstructure connected to good mechanical performances. A uniform distribution of a very fine Zn-based intermetallic phase, responsible of the self-hardening feature of the alloy was detected.
Addition of Mg up to 1% contribute to enhance the alloy mechanical performances and its resistance to the corrosive media.

1. Introduction

There is an increasing interest to employ light-weight materials to decrease energy consumption and emissions of gas in the environment [1]. This is a very important target and involves particularly transport industries. Aluminum alloys reveal important properties (low density, high strength stiffness to weight ratio, good formability and good corrosion resistance) and for this reason they are suitable for the manufacturing of components for automotive and aerospace applications [2-5].
It has been widely reported the great effort within the research community to develop new alloys and/or innovative processes for the production of high performance industrial components. Semi-solid processes (thixoforming, rheocasting) [6-10] and some innovative technique, such as advanced squeeze casting [11-15] have been considered as near net shape route able to reduce the presence of defects (shrinkage or gas porosity) generated usually in the conventional Al casting parts. Actually, high investments related to these processes delay their extensive industrial application.
An attractive option can be attributed to use of a "self-hardening" aluminum alloys [16]. This class of alloys has a particular characteristic: they are subjected to a natural ageing phenomenon and after a period of about 7 to 10 days can achieve a good final mechanical properties without any further thermal treatment [17-18]. This issue represents an important benefit contributing to reduce considerably the production cost of some components.

In this paper a self-hardening Al-based (AlZn10Si8Mg) alloy, produced by die-casting, with increasing Mg content has been produced and investigated. Comparison of three types of alloys, considering also the solidification rate, has been carried out with the aim to find an optimal composition and condition for good mechanical performance and good corrosion resistance achievements.

2. Experimental Procedures

The alloys, with the chemical composition reported in Table 1, have been produced by die casting technique in Teksid Aluminum Srl (Carmagnola, Torino-Italy).
Structural and mechanical properties, as well as corrosion resistance, as a function of Mg content have been investigated. Since the maximum solubility of Mg in Al is at 17.4% wt. under equilibrium condition, the Mg content usually does not exceed 5% in wrought alloy and does not exceed 10% in cast alloy. For these reasons in this investigation the Mg content is maintained in this range.
The alloys produced, with an increasing Mg content have been labeled as Sample 1 for AlZn10Si8Mg alloy, Sample 2 for AlZn10Si8Mg1 alloy and finally Sample 3 for AlZn10Si8Mg3 alloy, as reported in Table 1.

Table 1 Chemical composition (wt. %) of the three alloys produced

Elements	Si	Fe	Cu	Mn	Mg	Zn	Ti	Al
Sample 1	7,5-9,5	0,30	0,10	0,15	0,2-0,5	9,0-10,5	0,15	bal.
Sample 2	7,5-9,5	0,30	0,10	0,15	1,0	9,0-10,5	0,15	bal.
Sample 3	7,5-9,5	0,30	0,10	0,15	3,0	9,0-10,5	0,15	bal.

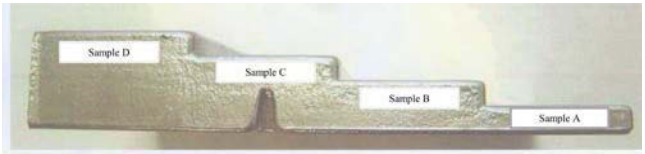

Figure 1. Step casting geometry used for the study.

To analyse the effect of the solidification rates on the microstructure of the casting for all compositions considered a special geometry, presented in Figure 1, has been developed.
The weight of the aluminium alloy casting, without runner system is about 0.5 kg.

The above mentioned configuration allows obtaining casting with different solidification rates with different microstructure development in the produced casting. In this step casting a range of thickness going from 5 to 20 mm has been generated and the solidification rate decreases from zone A (close to the runner) to zone D (close to the riser) providing a diverse microstructural behavior in the casting.
The alloys mechanical performances have been investigated using some samples extracted directly from the prepared configuration. In particular, samples (50mmx10mmx5mm) coming from zone A and C have been employed for the determination of their flexural stress and flexural strain at break through three point bending test (Dynamometer Zwick Z100 tool). Due to the dimensions of the samples, which are not appropriate for tensile test, three point bending test method has been adopted. The applied load corresponds to 5 KN.
For impact test samples extracted from zone B and D have been employed, in order to monitor the energy absorbed by the samples during fracture. Charpy pendulum, 50 J at room temperature, and un-notched samples with standard dimension (10mmx10mmx55mm) have been used for the test.
On the polished samples hardness measurements have been performed using a Volpert DU01 tester. A force of 50 N has been applied for 15 s for each measurement and a minimum of 5 indentations were performed on each samples.
Samples for morphological analysis, have been extracted from those tested from mechanical point of view and then have been prepared by a standard metallographic technique by mounting and polishing procedures. The microstructure of the samples has been investigated using an optical microscope, (OM, MeF4 Reichart-Jung) and Scanning Electron Microscopy (SEM, Leo 1450VP) equipped with Energy X-rays Dispersive Spectroscopy unit (EDS, Oxford microprobe) used for compositional analysis. The same instrument has been used for fracture surface analysis carried out on the fractured surfaces, after mechanical tests, to determine some causes related to the samples failure.
X-ray technique (X-ray, PANanalytical tool with Cu K_α wavelength of 1.5418 Å) has been employed for phase identification.
Corrosion test in a salt spray chamber has been carried out according to the Standard ISO 9227 using the whole configuration, with all compositions, to check the effect of Mg on the corrosion resistance of the alloys. Following the visual inspection of the whole configuration, some samples have been extracted directly from the step casting piece and then have been submitted to some mechanical properties assessment to compare the alloys behaviour prior and after corrosion test. The corrosion resistance has been monitored for all the three alloys inserting into the test chamber containing the corrosive media (the solution used was NaCl 5wt%) for 480 hours as provided by the Standard. The chamber was maintained at a temperature of 35°C for the entire test period.

3. Results and discussion

Microstructure analysis

The solidification is critical for the development of the microstructure in the casting and can be considered as a responsible for the mechanical properties development. The solidification can be divided principally into two stages: firstly the primary α-Al phase and the eutectic regions have been developed followed by the separation of the secondary intermetallic particles from the melt. The effects of the cooling rates and as consequence of the increased solidification rates within the cast micro-structure generally are able to avoid the development of segregation, considerable phase dispersion.
The alloys with different solidification rate and different Mg content have been submitted to morphological observation. The microstructure of all studied alloys consists in α-Al precipitates originated from the liquid metal as primary phase. This solid solution is immersed in the Al-Si eutectic mixture.
Figure 2 reports the microstructure of the alloys as a function of Mg content and solidification rate. In particular, the condition reported, for comparison, corresponds to the alloys extracted from zone A and C, with high and slow solidification rate, respectively.
Independently from the Mg content, high solidification rate promotes a rapid nucleation and growth of the particles and the development of a finer particles/microstructure. Due to the rapid solidification the primary α-Al phase cannot grow up to a full dendritic morphology prior to a total solidification of the melt. In particular, a finer microstructure has been observed for samples coming from zone A (with the highest solidification rate, left hand side in Figure 2) compared to zone C (with the lowest solidification rate, right hand side in Figure 2).

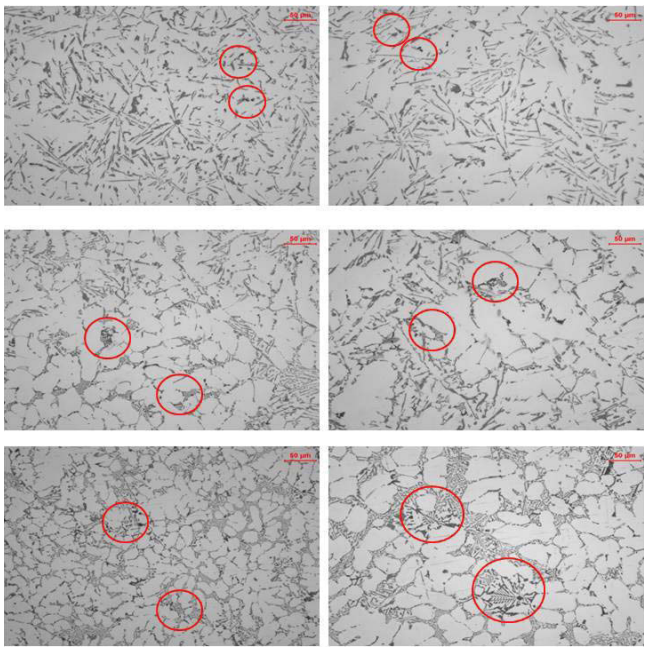

Figure 2. Microstructure of the alloys considered as function of Mg content and of solidification rate, left hand side samples type A, right hand side samples type C.

The morphology of the samples results to be governed by the Mg content. As Mg percentage increases (passing from the top of the figure to the bottom) the development of a more accentuated dendritic morphology can be observed, the structure growths into the formation of α-Al in form of dendrites associated to some more highlighted segregation of the eutectic regions (moving from top to bottom in Figure 2). In the case of a modest amount of Mg the microstructure shows an acicular features. At comparable positions among the castings no considerable variation has been evidenced.
In all alloys Mg based intermetallics with a Chinese-script morphology (areas evidenced in Figure 2) has been detected. The dimension of the Mg_2Si compounds can be directly correlated to

the Mg content in the alloy: as expected higher percentage of Mg leads to the enlargement of Mg_2Si particles. At the same time, the solidification rate controls the growth of the intermetallic particles: in the case of samples extracted from zone C with lower solidification rate the largest precipitates have been developed. A relatively equivalent condition has been obtained with high Mg content and low solidification rate..

Figure 3 reports the spectra obtained by X-Ray analysis. Some differences have been evidenced: in all alloys considered the presence of α-Al and Si has been detected, but the diffraction signals related to the presence of Mg_2Si secondary phase are more accentuated in the case of AlZn10Si8Mg1 and AlZn10Si8Mg3 alloys compared to the AlZn10Si8Mg alloy. The presence of $MgZn_2$ intermetallic phases has been also detected.

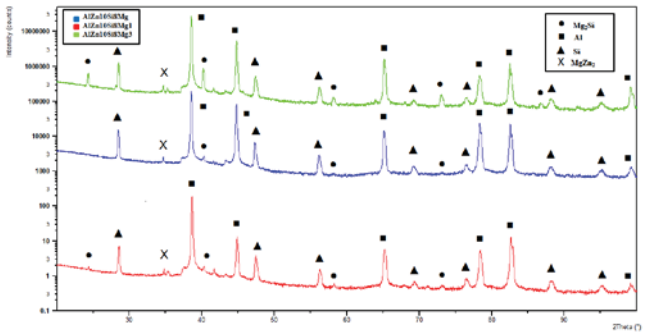

Figure 3. X-Ray diffractograms for the studied alloys.

The presence of Zn- based (bright white particles in Figure 4) and the hexagonal α-AlFeMnSi intermetallic particles (grey particles in Figure 4) have been detected by SEM observation and EDS analysis which interrupt randomly the microstructure of the alloy for all compositions. Zn has been subjected to a diffusion process responsible of the self-hardening behaviour of these type of alloys. The diffusion process seems to be stabilized after 20 days, no significant differences have been detected after this period, as microstructure and mechanical behaviour regards. Even if iron is generally considered as unfavourable impurity in the casting, it has been maintained at low level and in the presence of Mn, which has the capacity to alter the morphology of the intermetallics, the promotion of the formation of a more compact α-AlFeMnSi intermetallic particles has been performed. In this way the negative effect on the mechanical properties (in particular as ductility concerns) and on the corrosion resistance has been limited. As Mg content increases the development of $MgZn_2$ intermetallic particles is highlighted as indicated in Figure 5. In this microstructure $MgZn_2$ intermetallic particles are near to the AlZn intermetallics. Migration of Zn has been occurred within the grain boundary and a diffusion of this element to produce $MgZn_2$ intermetallics has been observed.

Mechanical properties evolution

In Figure 6 the energy absorbed by the un-notched samples has been reported. At high solidification rate there are no differences between the energy absorbed in the samples during fracture. Even if, the Mg content increases in such situation, the intermetallic particles present a small dimensions and, due to the their uniform distribution within the microstructure, no negative effect on impact resistance has been produced. When the solidification rate decreases and Mg content increases, due to the development of a coarser microstructure with larger intermetallic particles the impact energy of the samples has been considerably decreased.

Superior hardness has been measured in the case of Mg rich alloys due to the growth of hard intermetallic particles within the structure.

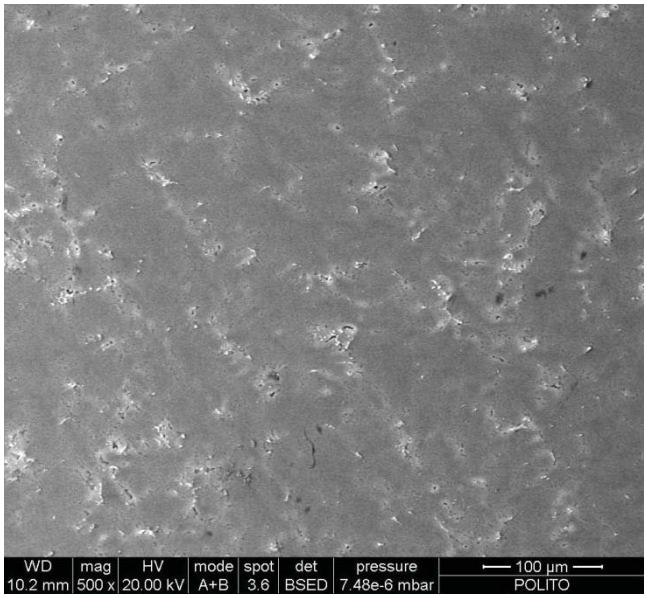

Figure 4. SEM microstructure of the AlZn10Si8Mg alloy showing the presence of Zn and Fe-based intermetallic particles.

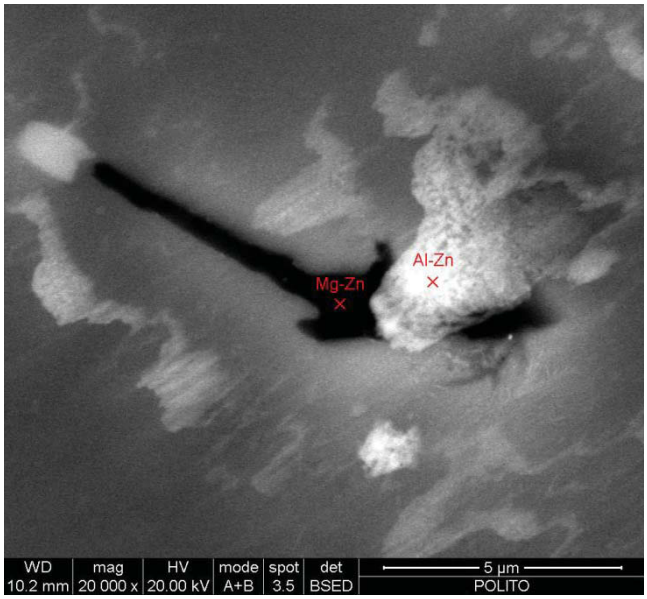

Figure 5. SEM microstructure showing the presence of the intermetallic particles in the as -cast sample.

In the case of the highest Mg content, as solidification rate decreases, a locally amplification of this property has been obtained. Figure 7 reports the results of a three point bending test carried out on the samples. Sample B with 1% of Mg shows an enhanced flexural stress at break compared to Sample A for both microstructures with high solidification rate and low solidification rate, respectively, due to the strengthening effect of Mg_2Si intermetallic particles. The further increase of Mg content,

determines a rapid decrease of the flexural stress at break for both microstructures as a consequence of the evolution of a large precipitates. These precipitates, mostly due to their large size, contribute to the crack developments and consequently to the failure of the alloy. The same trend, a drastic reduction has been obtained as the flexural strain at break concerns.

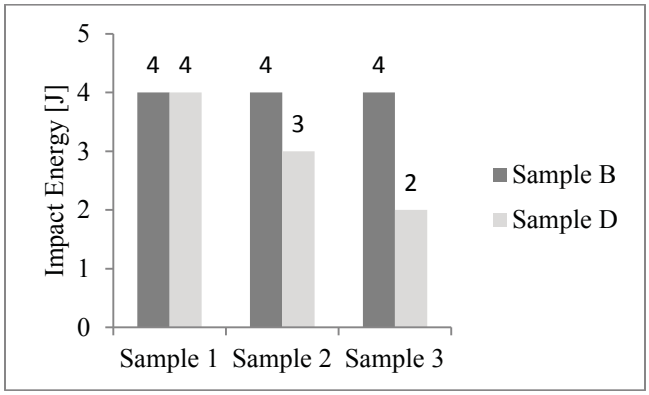

Figure 6. Impact Energy for the alloys investigated.

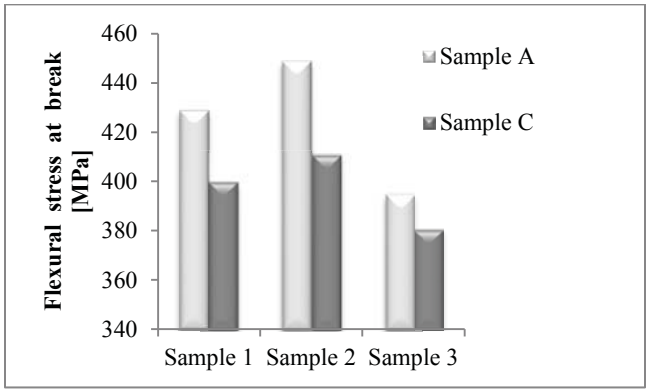

Figure 7. Flexural stress at break for the alloys investigated.

On the fractured surfaces fracture surface analysis has been performed. Different types of defects have been accidentally detected with a limited effect on the alloys mechanical properties evolution. Figures 8-10 report the fracture surfaces of the alloys: in all cases a mixed type of fracture has been illustrated characterized by some dimples and cleavage fracture regions.
The presence of aluminium porosities (Figure 8), shrinkage porosities (Figure 9) and the presence of some brittle particles (Figure 10) have been occasionally observed.

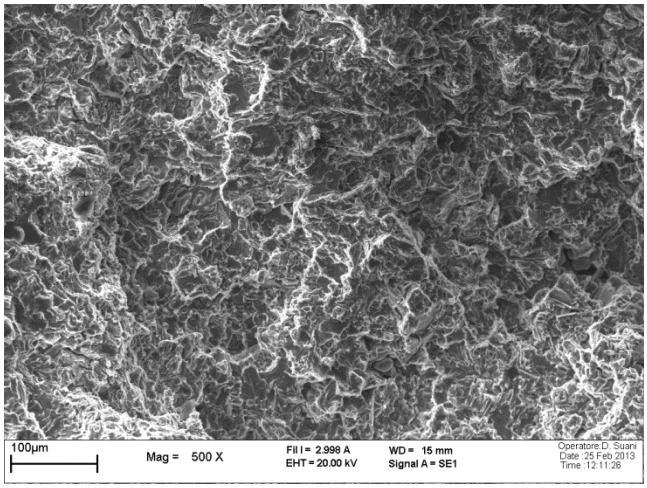

Figure 8 SEM fractographs of Sample 1.

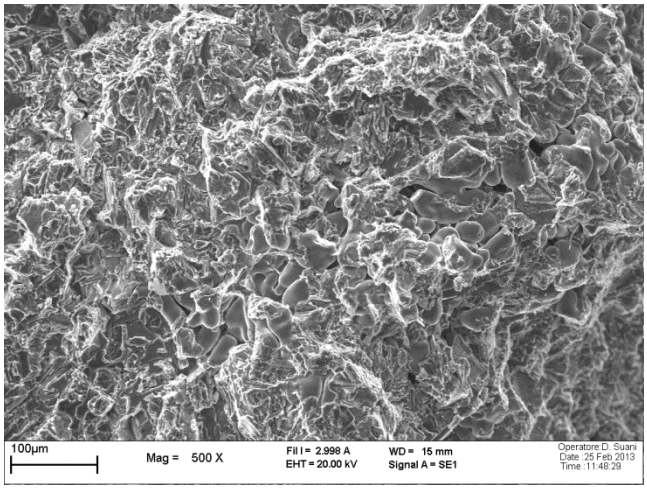

Figure 9. SEM fractographs of Sample 2.

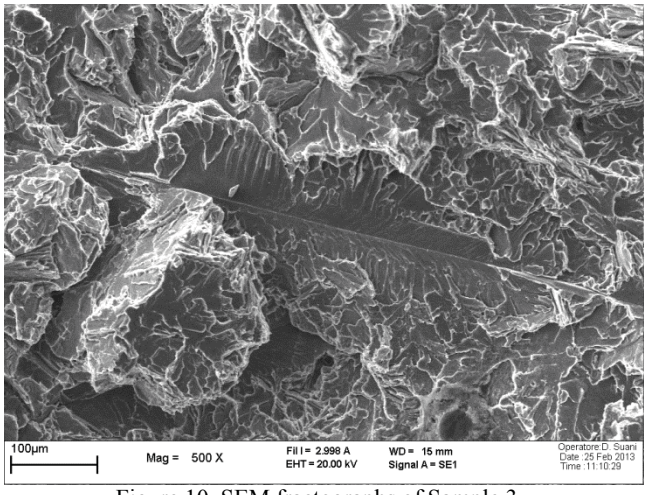

Figure 10. SEM fractographs of Sample 3.

Corrosion resistance investigation

The corrosion resistance capability of the alloys have been monitored over 20 days during immersion in the corrosive medium, as represented in the image in Figure 11. At pre-set time the samples have been extracted from the batch in order to check the degradation level and to assess if the corrosion is only a surface phenomenon or involves the complete metal matrix. Comparison of the samples has been realized to verify the effect of the Mg addition on the corrosion resistance of the alloys. Figure 12 shows the images attained after the maintenance for 24, 168 and 480 hours in the corrosive ambient. After 480 hours of exposure the samples are no longer detected.

After 24 hours of exposure, the alloys with a higher content of Mg seems to be more resistant to the corrosive environment: at the end of the corrosion test the exposed surface is more or less identical to the original one. Some preliminary mechanical analysis carried out on some samples removed from those exposed to the corrosion test are very promising: in fact, the mechanical performance after corrosion test are quite equivalent to those obtained previous to corrosion test, meaning that the some minor changes involve only the surface of the alloy and does not affects their general mechanical behaviour.

Figure 11. Set-up of the corrosion batch for the experiment

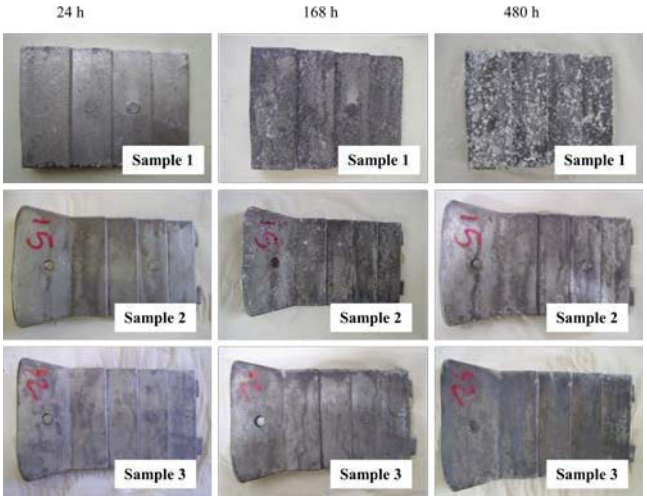

Figure 12 Photos of the samples analysed in the corrosive medium

At the end of the corrosion test no variation of the impact energy has been achieved for the alloys obtained with high solidification rate.

4. Conclusions

In this paper AlZn10Si8Mg alloys with increasing Mg content were studied. The effect of the solidification rate on the alloys performances was investigated. Based on the results obtained up to now the following conclusions can be drawn:

1. as it is well known, the solidification rate has an important effect on the microstructural evolution: higher solidification rate favours the development of a finer microstructure connected to higher mechanical performances;
2. at low solidification rate, as a consequence of the development of larger Mg_2Si particles, lower impact energy was measured, while concerning flexural stress at break alloying with 1% of Mg seems to be a good option; increasing the Mg content up to 3% a negative effect was achieved;
3. apart from the solidification rate, high Mg content reduces the flexural strain at break of the alloys;
4. at the end of the corrosion test the impact energy was measured; in the case of alloys obtained with high solidification rate no variation of the mechanical properties was recorded;
5. combining the mechanical properties development and the corrosion resistance of the alloy it has been found that a rapidly solidified self-hardening AlZn10Si8Mg1 alloy appears a good candidate for automotive component production.

5. References

1. J.D.Du, W.J. Han,Y.H. Peng, C.C. Gu,*"* Potential for reducing GHG emissions and energy consumption from implementing the aluminum intensive vehicle fleet in China*", Energy* 35 (2010), 4671- 4678.
2. J.Hirsch, T.Al-Samman, " Superior light metals by texture engineering: Optimized aluminum and magnesium alloys for automotive applications ,"*Acta Materialia,* 61 (2013), 818–843.
3. Z.Huda, N. Iskandar Taib, T.Zaharinie," Characterization of 2024-T3: An aerospace aluminum alloy, *"Materials Chemistry and Physics,*113 (2009),515–517.
4. L.Lang, T.Li, D.An, C.Chi, K.B.Nielsen, J.Danckert, " Investigation into hydromechanical deep drawing of aluminum alloy-Complicated components in aircraft manufacturing," *Materials Science and Engineering* A 499 (2009), 320–324.
5. R.Ramesh, R.Bhattacharya, G.Williams, " Effect of ageing on mechanical behaviour of a novel automotive grade Al-Mg-Si alloy," *Materials Science and Engineering* A, 541 (2012), 128–134.
6. H.Lakshmi, M.C.Vinay Kumar, Raghunath, P.Kumar, V. Ramanarayanan, K.S.S. Murthy, P. Dutta, " Induction reheating of A356.2 aluminum alloy and thixocasting as automobile component," *Trans. Nonferrous Met. Soc. China*, 20(2010), 961-967.
7. A. Neag, V.Favier, R.Bigot, M. Pop," Microstucture and flow behaviour during backward extrusion of semi-solid

7075 aluminum alloy," *Journal of Materials Processing Technology* 212 (2012), 1472–1480.
8. L. Bochao, P.Youngkoo, D.Hongsheng, " Effect of rheocasting and heat treatment on microstructure and mechanical properties of A356 alloy," *Materials Science and Engineering* A, 528 (2011), 986–995.
9. G.Wallace, A.P. Jackson, S.P. Midson, Q.Zhu, " High-quality aluminum turbocharger impellers produced by thixocasting," *Trans. Nonferrous Met. Soc. China*, 20 (2010), 1786-1791.
10. M. Rosso, I. Peter, "New frontiers for thixoforming," *Int. J. Microstructure and Materials Properties*, Vol. 8, Nos. 1/2, (2013).
11. M. Rosso, I. Peter, C. Bivol, R. Molina, G. Tonno, "Development of industrial components by advanced sqeeze casting," *Int J Mater Form*, (2010) Vol. 3 Suppl 1,787–790.
12. M. Rosso, I. Peter, R. Molina, A. Montedoro, G. Tonno, P. Claus, "Aluminum based components with enhanched characteristics through advanced squeeze casting process," *La Metallurgia Italiana* - n. 3/2012.
13. Z. Ming, Z. Wei.Wen, Z. Hai-Dong, Z. Da-Tong, Li Yuan-Yuan," Effect of pressure on microstructures and mechanical properties of Al-Cu based alloy prepared by squeeze casting," *Trans. Nonferrous Met. SOCC. China,* 17(2007), 496-501.
14. Z.Han, X. Huang, A. A. Luo, A. K. Sachdev, B.Liu," A quantitative model for describing crystal nucleation in pressurized solidification during squezze castign," *Scripta Materialia*, 66 (2012), 215–218.
15. P.Vijian, V.P. Arunachalam, " Optimization of squeeze casting process parameters using Taguchi analysis," I*nt J Adv Manuf Technol* (2007) 33, 1122-1127.
16. E.Tillova', E.Durinikova, M.Chapulova, " Structural analysis of secondary AlZn10Si8Mg cast alloy," *Acta Metallurgica Slovaca*, Vol. 17, 2011, No. 1, p. 4-10.
17. M. Azadi, M.M. Shirazabad, " Heat treatment effect on thermo-mechanical fatigue and low cycle fatigue behaviors of A356.0 aluminu alloy," *Materials and Design*, 45 (2013), 279–285.
18. I.A. Luna, H.M. Molinar, M.J. Castro Roman, J.C. Escobedo Bocardo, M.Herrera Trejo, "Improvement of the tensile properties of an Al–Si–Cu–Mg aluminum industrial alloy by using multistage solution heat treatments," *Materials Science & Engineering*, A 561 (2013) 1–6.